Anbar Journal of Engineering Science (AJES)
P-ISSN: 1997-9428 ; E-ISSN: 2705-7440

Vol. 13 , No. 1 (2022) , pp. 1 ~12
DOI: https://doi.org/10.37649/aengs.2022.175875

Unviersty of Anbar

Anbar Journal of Engineering Science©

journal homepage: https://ajes.uoanbar.edu.iq/

Experimental Investigation of the Optimum Angle for the Hybrid PV/T Collector

Zuhair D. Mohammed [a], Saad M. Jalil [b]

[a] *Municipalities Directorate of Anbar/ Fallujah / Iraq*
[b] *Department of Mechanical Engineering/ University of Anbar / Iraq*

PAPER INFO

Paper history:
Received 27/12/2021
Revised 24/01/2022
Accepted 12/02/2022

Keywords:
electrical power, optimum inclination angle, PV/T collector, thermal efficiency

ABSTRACT

In this article, an experimental study of the single-pass hybrid (PV/T) collector is conducted in the climatic conditions of Fallujah city, where the experimental results are compared with a previous research to validate the results. The effect of changing the angle of inclination of the hybrid collector (PV/T) and its effect on the electrical power in the range (20°-50°) is studied. The optimum angle of the collector is found to be 30°, which gives a maximum electrical power of 58.8 W at average solar radiation of 734.35 W/m^2. In another experimental study with different air flow rates ranged from 0.04 kg/s to 0163 kg/s, where it is found that the maximum electrical power of 57.66 W at an air flow rate of 0.135 kg/s, while the maximum thermal efficiency reaches 33.53% at an air flow of 0.163 kg/s at average solar radiation of 786 W/m^2.

1. Introduction

Most of the Iraqi cities suffer from a lack of electricity supply, because of their dependence on burn-ing fossil fuels, which is not enough to cover the shortage of electric power. Fossil fuels cause envi-ronmental pollution in addition to increasing global warming, so the world has resorted to thinking about clean energy to generate electric power, in-cluding the adoption of photovoltaic cells or winds to generate energy. Joshi et al. [1] presented a hy-brid solar air collector (PV/T) study to compare electrical and thermal performance. They concluded through experiments that a collector containing PV panels from glass to Tadler has lower electrical efficiency than a collector containing PV panels from glass to glass. They also showed that the overall thermal efficiency increases with increasing air velocity and decreases with increasing collector length. Sarhaddi et al. [2] studied the PV/T air system to test electrical and thermal performance. An electrical model was used and developed to calculate the voltage and current, and a thermal model was developed to calculate the outlet air temperature and the temperature of the solar panels. Through the study, the researchers found that the electrical and thermal efficiency were (10% and 17%), respectively. Tiwari et al. [3] conducted a theoretical and experimental study of the hybrid solar air collector (PV/T). It was proven through the study that there was a fair agreement between the theoretical and experimental results. They also found an increase in the overall efficiency of the system by about (18%). Kasaeian et al. [4] published an experimental study of the single-path hybrid system and found through the study that the thermal efficiency increased with a decrease in the

* Corresponding author: Saad M. Jalil ; saad.jalil@uoanbar.edu.iq ; +9647800842666

depth of the channel and increased with an increase in the flow, as the thermal efficiency reached (15% to 31%) for a flow rate of (0.018 kg/s to 0.06 kg). Amori and Al-Najjar [5] studied the hybrid collector theoretically. An improved electrical and thermal model of the collector was developed, where Matlab was used to solve the electrical and thermal model problems, and the researchers found that the model was more accurate in terms of error rates. The electrical and thermal efficiencies for a winter day reached (12.3%-19.4%), respectively, while the electrical and thermal efficiencies for a summer day reached (9%-22.8%), respectively. Amori and Abd-AlRaheem [6] published a study on a hybrid solar air collector (PV/T) to compare the electrical and thermal performance. Three hybrid collectors (PV/T) have been designed. The first type is a single channel with a double pass, the second type is a single channel with one pass, and the third type is a single channel with a single pass, and another photoelectric collector is designed without cooling. They found through the study that the first type gives a higher combined efficiency, while the third type gives a higher electrical efficiency. Ahmed and Mohammed [7] published a theoretical and experimental study of the effect of dust on the hybrid air collector (PV/T), and they found through the study that dust has an effect on the thermal efficiency as the efficiency decreased by (13.4%). The electrical efficiency for the clean collector was 10.2%, and the electrical efficiency for the collector, in the case of dust, was 5.6%. Pauly et al. [8] they conducted a numerical study of the PV/T system using ANSYS software. Through the study they found that there is a fair agreement between numerical and experimental results. The researchers also showed that the overall efficiency increases with increasing flow rate and decreases with increasing channel depth. Tonui and Tripanagnostopoulos [9] presented a study of the hybrid air collector (PV/T) using fins or metal sheets in the middle of the channel. The study showed an increase in thermal and electrical efficiency. Dubey et al. [10] conducted an analytical study of four types of hybrid (PV/T) collectors: the first type (PV glass-glass with channel), the second type (PV glass-glass without channel), the third type (PV-Tedlar glass with channel), and the fourth type (PV-Tedlar glass without channel). Through the study, they found that the first type has a higher electrical efficiency is compared to the other collectors. Fterich et al. [11] designed a hybrid (PV/T) system for the purpose of drying tomatoes. Forced convection was used to move air over and under the PV panels, increasing the thermal energy of the system that was used for the purpose of drying as well as increasing the electrical energy generated by the panels. Ali et al. [12] published a new study on the hybrid system (PV/T) using the solar pond system. A heat exchanger installed under the photovoltaic panels was used for the purpose of cooling the panels in addition to storing water in the storage area. The experiment was conducted in Iraq for a period of four months, where the daily electrical and thermal efficiency was reached in September at 30% and 9.3%, respectively. Ahmed and Mohammed [13] completed an experimental study of a dual-pass hybrid solar collector using porous materials. they concluded that the presence of porous materials improve the thermal energy of the system. The thermal and electrical efficiencies of the collector containing porous materials were (80.2% and 8.7%), respectively, and the thermal and electrical efficiencies of the collector without porous materials were (50.2% and 10.9%), respectively. Hadipour et al. [14] also published a paper on the cooling of photovoltaic panels using pulsed water of a hybrid collector (PV/T). The researchers pointed out that this type of system reduces the consumption of water needed for cooling and improves the electrical efficiency as compared to a system that does not use a cooling system. They found through experiments that the system that does not use a cooling system has an electrical efficiency of (9.1%) and a power output of (54W), and the panels' average temperature is (57.1C), while the steady/cooling system has an electrical efficiency of (12.1) and a power output of (72W), while the average temperature of the panels is (24.8 C). As for the system that works (pulsed/cooling) within a working cycle (DC = 1, DC = on time/off time), it has an electrical efficiency of (11.6%) and a power output of (25.7 W), and the average temperature of the panels is 26.5C. Jakhar et al. [15] published a study on hybrid (PV/T) collectors using water. The model was studied mathematically and compared experimentally. The heat exchanger was placed under the PV panels. The researchers found an increase in electrical efficiency of (1.04%-1.41%). Murad et al. [16] published a research article on the optimum angle of the photovoltaic cell for Baghdad, Diyala and Tikrit. The angle has been changed from 0° to 90°. Through the study, they concluded that the optimum angle for the photovoltaic cell for all the above-mentioned cities is 31°. In the same context, Al-Sayyab et al. [17] published a theoretical and experimental study on the optimal angle of the photovoltaic cell for the city of Basra. The angle has

been changed from 0° to 90°. It was found through the study that the optimal angle for the photovoltaic cell is 28°. Sharma et al. [18] published

India. The researchers stated that the solar tracking system is not useful due to the high cost. The angle was changed from 10° to 40°. It was found through the study that the annual optimal angle for the pho-tovoltaic cell ranges between 26-28°, which increases the electrical energy by 7-8%. The current a study on choosing the optimum angle for a photovoltaic cell within the Chandigarh site,

re- search article aims to study the inclination angle of the hybrid collector (PV/T) and its effect on the electrical power of the solar panel also aims to study the effect of increasing the mass flow on the thermal and electrical properties of the hybrid collector.

Table 1. Summary of previous studies

Study	year	Type of collector	Type of absorber	Implementation	Findings
[4]	2017	PV/T air collector	Flat plate absorber	Experimental of the hybrid collector	Thermal efficiency increases with the decreasing depth of the channel and also increases with an increased mass flow rate.
[5]	2012	PV/T air collector	Flat plate absorber	Simulation model of the hybrid collector	Improved thermal and electrical model was developed, and it turned out more accurate in terms of error rates.
[6]	2014	PV/T air collector	Flat plate absorber	Experimental of the hybrid collector	Double-channel with single-pass collector have higher combined efficiency.
[7]	2017	PV/T air collector	Flat plate absorber	Experimental of the hybrid collector with and without dust	Dust affects the thermal and electrical performance, as the overall efficiency decreased by 17.5%.
[8]	2016	PV/T air collector	Flat plate absorber	Simulation model of the hybrid collector	Reducing depth of channel increases overall efficiency
[11]	2018	PV/T air collector	Flat plate absorber	Experimental of the hybrid collector	Increase in electrical efficiency and the use outlet air for drying tomatoes
[12]	2020	PV/T water collector	Flat plate absorber	Experimental of PV/solar pond	Highest thermal efficiency of 30% and the highest electrical efficiency of 9.357%
[14]	2021	PV collector	Flat plate absorber	Experimental of PV using water spray	Reduces water consumption for cooling and improves electrical efficiency.
[15]	2017	PV/T water collector	Flat plate absorber	Experimental of a hybrid collector with heat exchanger	Increase in electrical efficiency by (1.04%-1.41%)
[16]	2018	PV collector	Flat plate absorber	Find of optimal inclination angle	The optimal inclination angle of the collector for the cities of Baghdad, Diyala, and Tikrit is 31°.

[17]	2019	PV collector	Flat plate absorber	Find of optimal inclination angle	The optimal inclination angle of the collector for the city of Basra is 28°
[18]	2020	PV collector	Flat plate absorber	Find of optimal inclination angle	The optimal inclination angle of the collector for the Chandigarh site, India ranged from 26°-28°.

2. Description of the System

A single-pass PV/T system is constructed as shown in Fig. 1, consisting of two PV panels connected in parallel. Descriptions of the hybrid collector and solar panels can be found in Tables 2 and 3. The panels are fixed over a 5 cm high wooden channel. The wood was chosen because it was easy to cut during the construction and was insulating and inexpensive. Air is supplied to the system using two fans (DC). The fans are installed inside a trapezoidal extended duct that has been attached to the inlet of the channel. In addition, another rectangular duct has been attached to the end of the channel to ensure uniform flow at the outlet for measuring the velocity. The system metal base is designed to allow the solar panels to tilt (change it its angle of inclination) from 0^o to 70^o.

Figure 1. A photograph of the system used in the study

Table 2. Specifications of Solar Panels

Solar panel type	Polycrystalline silicon
Out peak power (P_{max})	60 W
Max-power voltage (V_{max})	17.64 V
Max-power current (I_{max})	3.40 A
Open-circuit voltage (V_{oc})	21.16 V
Open-circuit current (I_{sc})	3.74 A
Max- system operating voltage	1000 V
Frame material	Aluminum
Operating temperature	25°
Solar radiation	1000 W/m^2

Table 3. Specifications of Hybrid (PV/T) Collector

Collector length	2860 mm
Collector width	580 mm
Collector height	70 mm
Collector inclination angle	20°,30°,40°,45°,50°
Thickness of glass wool insulation	10 mm
Type of collector	Flat collector
Thickness of wood	20 mm
Thermal conductivity of wood	K=0.059 W/m
Outlet area	540 mm*50 mm
Inlet area	260 mm*120 mm

3. Measurement

The Arduino (Mega2560) is installed in a plastic case measuring (20 cm * 20 cm), which contains 52 digital inputs and 16 analog inputs. The Arduino is programmed by the system (ID) to transmit data to the computer as in figure (1). The thermocouples are connected to the Arduino by connecting the two ends of the thermocouple to an electronic part (MAX6675) to convert the voltage from millivolts to 5 volts because the Arduino operates at 5 volts. A K-type thermocouple with a length of 2 m is used

in the range (-270°C-1260°C). Two thermocouples are installed in the middle of the beginning and end of the duct, as well as four thermocouples mounted on the surface of the PV panels, four thermocouples on the back side of the panels, one thermocouple for measuring ambient temperature, and two thermocouples for measuring the temperature of the inner and back surface of the wood. Figure (2) shows the distribution of thermocouples for the hybrid collector. A meter is used to measure the incident solar radiation type (SM206) with a measuring range of (1-399.9) W/m^2, and a hot wire (anemometer) is used to measure the air velocity in the channel with a measuring range (0-30 m/s). The speed of the fans is changed by a speed regulator, an electronic (DC) device operating at a variable voltage (1.25-12 V) that provides the possibility of changing the voltage for the purpose of controlling the desired speed. The type of thermocouple (k) used in this study is calibrated and compared with a mercury thermometer as shown in Fig. (3).

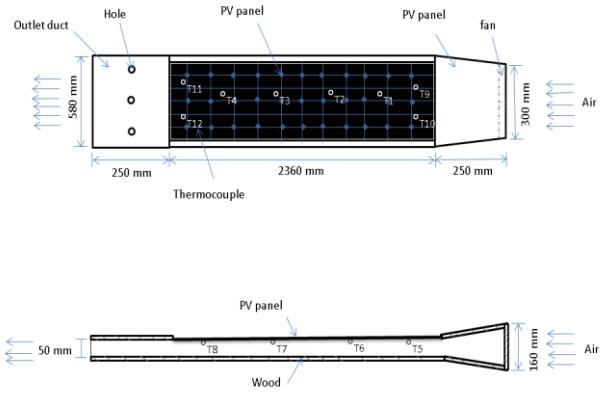

Figure 2. PV/T collector (a) top view, (b) cross-section

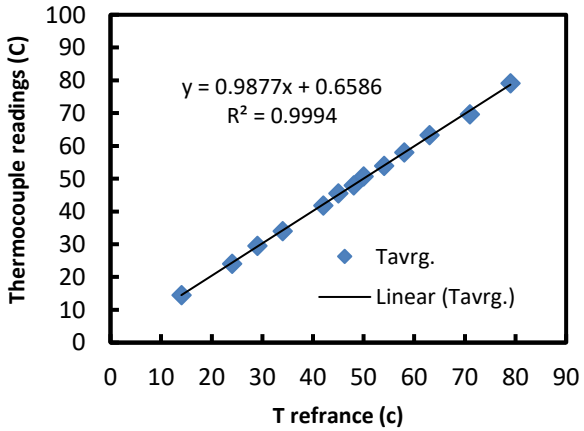

Figure 3. Thermocouples calibration

4. Electrical Loading System

Three loads are connected in series, each with a (1 ohm, 50 watts), and each is installed on the heat sink with a (DC) fan to cool the loads. Voltage and current are measured with and without a load, as shown in Figure (4), using a device (Digital multimeter) of the type (VICTOR VC 890C +).

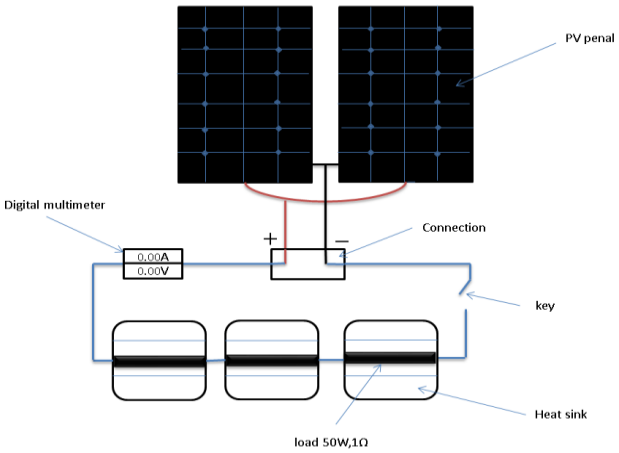

Figure 4. Electrical loading system

5. Statistical Analysis

5.1. Uncertainty Analysis

Every measured uncertainty of parameter leads to an accumulation of inaccuracy in all estimated parameters. The Root Sum Squares (RSS) uncertainty approach may be used to determine the propagation of error for (n) computed parameters, Xi, in a certain objective function, R [19]:

$$U_{RSS} = \sqrt{\sum_{i=1}^{n} \left(\left(w_i \frac{\partial R}{\partial x_i} \right)^2 \right.} \qquad (1)$$

Where w indicates total uncertainty by each parameter xi.

Table 4. The uncertainty values in parameters and calculation

parameter	Uncertainty
Reynolds no.	±3.46%
Thermal eff.	2.84 %
Electrical eff.	±0.203 %

Table 5. The Accuracy values of equipment

Equipment	Range	Resolution	Accuracy
Thermocouple type K	-270 to1260 °C	1 °C	± 1.4 °C
Multimeter DC voltage	200mV/2V/20 V/200V/1000 V	-	± 0.5%
Multimeter DC current	200µA/20mA /200mA/20A	-	± 1.2%
Thermal anemometer	0-30 m/s	0.01 m/s	± 3%
Solar power meter (SM206)	0.1-399.9 W/m^2	0.1W/m2	±10 W/m^2

5.2. Percentage Deviation (e) and Linear Coefficient of Correlation (r)

Statistical analysis is used to find the root mean square of the percentage deviation (e) and the linear coefficient of correlation (r) as follows [1] [5]:

$$= \sqrt{\frac{\sum(e_i)^2}{n}} \quad (2)$$

W*here,*

$$e_i = \left[\frac{x_i - y_i}{x_i}\right] * 100 \quad (3)$$

Where **xi** and $\boldsymbol{yi}$ denote simulated and experimental values, respectively.

$$r = \frac{\mathrm{n}(\sum \mathrm{x} * \mathrm{y}) - (\sum \mathrm{x}) * (\sum \mathrm{y})}{\sqrt{\mathrm{n} * (\sum \mathrm{y}^2) * (\sum \mathrm{y}^2)} * \sqrt{\mathrm{n} * (\sum \mathrm{x}^2) * (\sum \mathrm{x}^2)}} \quad (4)$$

Table 6. Comparison of experimental validations.

Parameter	Present work with [1]		present work with [5]	
	e %	r %	e %	r %
$T_{solar\ cell}$	10.93	0.91	Not given	Not given
$T_{back\ sur.}$	8.75	0.91	Not given	Not given
$T_{ave.cell}$	Not given	Not given	0.99	2.52

6. Variable Parameters Calculation

6.1 Thermal Efficiency: The thermal efficiency of (PV/T) system can be calculated from experimentally measured data and as follows [1] [2]:

$$\eta_{th} = \frac{\dot{m}cp(T_{out} - T_{in})}{A_p G} \quad (5)$$

$$\boldsymbol{\dot{m} = \rho V_a A_s} \quad (\mathbf{6})$$

6.2 **Electrical Efficiency:** The electrical efficiency of (PV/T) system can be calculated from experimentally measured data and as follows [6][20]:

$$\eta_{ele} = \frac{P_{pv}}{A_{pv} G} \quad (7)$$

$$P_{pv} = P_{load} + P_{fans} \quad (8)$$

$$P_{load} = I_{load} * V_{load} \quad (9)$$

$$P_{fans} = I_{fans} * V_{fan} \quad (10)$$

6.3 **Pressure Drop:** The following equation is used to calculate the pressure difference due to the lack of accurate devices because the pressure difference is small [21]:

$$\Delta p = \Delta p_f + \Delta p_{other} \quad (11)$$

$$\Delta P_f = \frac{\rho}{2} . f . \frac{{v_a}^2}{D_h} . L \quad (12)$$

$$f = \frac{0.079}{Re_D^{0.25}} \quad (13)$$

ΔP_{other}can also be found as follows:

$$\Delta P_{other} = \frac{1}{2} . K_l . \rho . {v_a}^2 \quad (14)$$

$$K_l = k_{exit} + K_{bend} + K_{entrance} \quad (15)$$

These values are (0.5, 1, and 2.2) respectively

The Reynolds number can be calculated as follows:

$$Re = \frac{\rho . v_a . D_h}{\mu} \quad (16)$$

$$D_h = \frac{2bh}{(b+h)} \quad (17)$$

7. Experimental Procedures

Before each experiment, the solar panels are cleaned of dust, as this affects the reduction of electrical and thermal efficiency. In addition, make sure that all the thermocouples used are connected and do not slip out of place because this affects the accuracy of the readings. The system operates from 7 a.m. to ensure a steady state and then takes readings starting from 8 a.m. to 5 p.m. The temperatures are recorded by Arduino with thermocouples type K, which include measurement of solar cell temperature, back surface temperature of PV, ambient temperature, and inlet and outlet temperature. Solar radiation is also measured with a solar power meter. In addition to using an anemometer (hot wire) to measure the air velocity in the channel, a millimeter is also used to measure voltage and current with and without load. The accuracy of the devices used in the current research is included as in table (5).

8. Results and Discussion

8.1. Experimental Validation

It is important to compare the experimental results of the current work with previous research to ensure the validity of the results. An experiment is conducted on April 6, 2021, on a clear day in the city of Fallujah, located at latitude 33.3°N and longitude 43.7°E, at an angle of inclination of 40° at Reynolds No. 9780.88 and compared by Joshi et al. [1] under the climatic conditions of New Delhi. Fig. (5) shows a validation of the experimental results of the current work with Ref. [1] on the temperature of the solar cell, and it has been found that there is a large agreement in terms of behavior, as we notice an increase in the temperature of the solar cell until midday, and then it decreases due to the decrease in solar radiation, Fig. (6) shows a validation of the experimental results with Ref. [1] on the back surface temperature of PV, where a fair agreement is observed between them in terms of behavior. The values of r and e have been compared with Ref. [1] as in table (6).

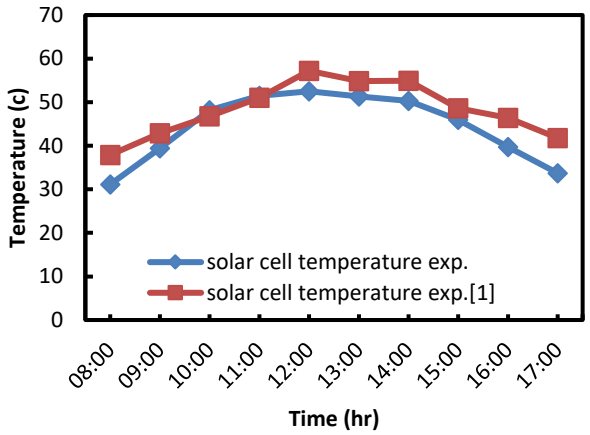

Figure 5. Hourly validation experimental solar cell temperature

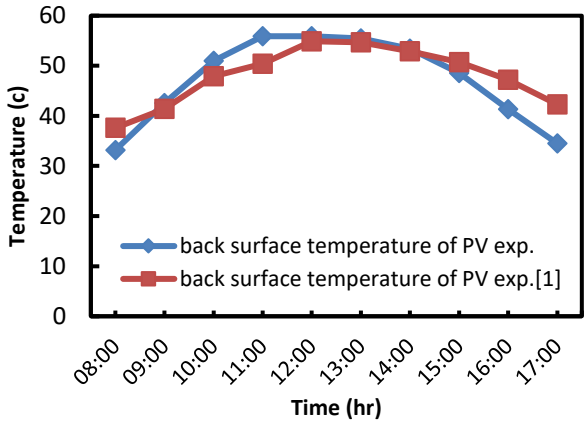

Figure 6. Hourly validation experimental back surface temperature

Fig. (7) shows a validation of the results for the open circuit current and the open circuit voltage for the current research with the Ref. [1], where it is noted that the current depends on solar radiation. As the radiation increases, the current increases with it, reaching the maximum values of the current at 12:00 and then it decreases due to a decrease in solar radiation. As for the voltage, it decreases with the increase in solar radiation, and it becomes clear through the comparison that there is a fair agreement in terms of behavior and that the reason

for the difference is due to the difference in solar radiation.

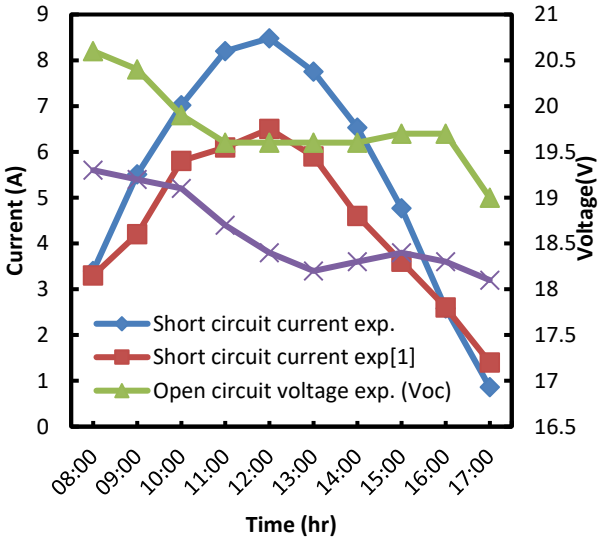

Figure 7. Hourly validation experimental short-circuit current and open-circuit voltage

An experiment was also conducted on May 24, 2021, with a Reynolds number of 6972.15, and it has been compared with the simulation results by Amori and Al-Najjar [5] under the climatic conditions of Fallujah city. Fig. (8) shows the comparison of the average solar cell temperature for the current research by Ref. [5], and it is found that there is a great agreement in terms of the behavior. The values of r and e have been compared with Ref. [5] as in table (6). Fig. (9) shows a comparison of the results for the thermal efficiency of the current research by Ref. [5], where it is noted that there is agreement and that the reason for the difference is that they relied in their simulations on the assumption that the ambient temperature is the same as the inlet temperature, which is not possible under the experimental conditions. In addition, they used a lower Reynolds number.

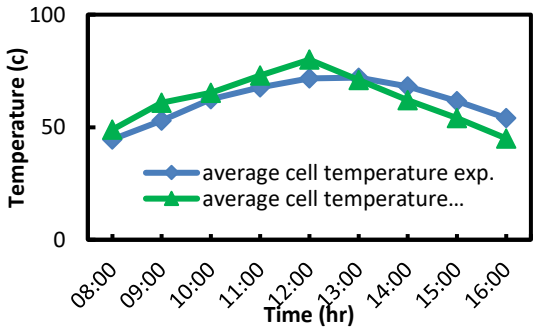

Figure 8. Hourly validation experimental and simulated of average cell temperature

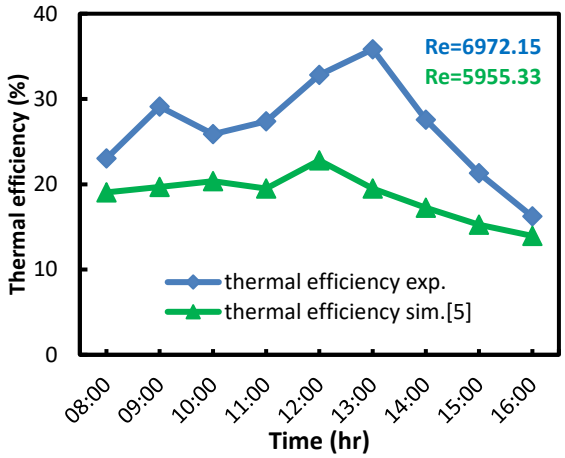

Figure 9. Hourly validation experimental and simulated of thermal efficiency

Figure (10) shows a comparison between the experimental results of the current work in terms of electrical efficiency by Amori and Abd-AlRaheem [6] under the climatic conditions of the city of Fallujah. The figure below shows that there is fair agreement in terms of behavior, and the reason for the difference is that the researchers in the Ref. [6] used a dual-path PV/T system, so there has been more cooling.

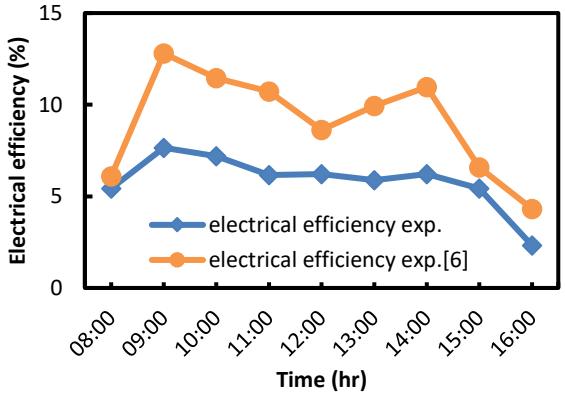

Figure 10. Hourly validation experimental of the electrical efficiency

8.2. *Cases Studied*

8.2.1. *Cases Study (I)*

Experiments were conducted to determine the optimum angle of the hybrid collector (PV/T) during the month of May for the period from 17th to 22nd,2021, where different angles of inclination of the compound were taken during this period, which were (50°, 45°, 40°, 30°, 20°). Figure (11) shows the effect of changing the angle with the maximum daily electrical power. It is clear through the study that the maximum electrical power is at

the angle of 30°, as shown in table (7). It is also clear from the figure below that the maximum daily solar radiation rate reached at the angle at 50°, which led to a decrease in electrical power due to the high temperature of the solar panels.

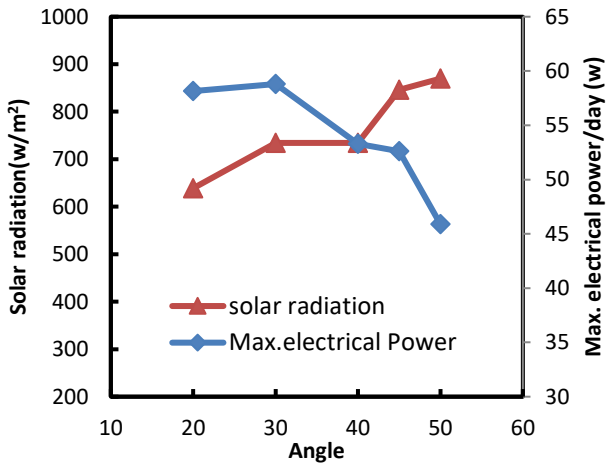

Figure 11. Variation of inclination angle and solar radiation with electrical power

Table 7. inclination angle and Solar Radiation with Maximum Daily Electrical Power

Angle	Average solar radiation (W/m^2)	Average Max. electrical power (W)
20°	638.9	58.16
30°	734.35	58.8
40°	734.3	53.3
45°	845.95	52.61
50°	869.7	45.88

8.2.2. *Cases Studied*

Experiments are conducted on the 30th and 31st of May and the 1st, 2nd, 3rd, and 5th of June to determine the effect of changing mass flow rate on the thermal and electrical properties of the hybrid collector (PV/T) under the climatic conditions of Al-Fallujah. The air velocity in the duct is adjusted in the range from 1.374 m/s to 5.499 m/s by varying the fan voltage to obtain flow in the range of 0.04 kg/s to 0.163 kg/s at Reynolds numbers 6926.26 to 28560.62. Table (8) shows the weather data for the days during which the solar radiation and ambient temperature experiments were conducted. Figure (12) shows the effect of changing mass flow rate on thermal efficiency, total efficiency, and electrical efficiency. It is observed that when the mass flow increases, the thermal efficiency also increases due to the increase in convective heat transfer, where the maximum thermal efficiency reached 33.53% at the highest mass flow of 0.163 kg/sec. Also, increasing the mass flow rate improves electrical efficiency, but does not have a significant effect, with a maximum electrical efficiency of 4.88% at a mass flow rate of 0.135 kg/sec. Figure (13) shows the electrical power produced by the hybrid system, which includes the electrical power consumed by the fans and the electrical power supplied to the load. It is seen that the power consumed by the fan increases with the increase in the mass flow rate. This is normal because the fan needs higher voltage and current when the flow is increased, and the maximum electric power supplied to the load is 57.66 W with a mass flow rate of 0.135 kg/s. For the pressure drop, the equations in Section 6.3 have been used to find it, under the range of the Reynolds number used in the current research, which corresponds to [20]. Figure (14) shows the effect of the mass flow rate on the pressure drop, as it is noted that the pressure drop increases with the increase in the mass flow rate and the maximum pressure drop reaches 66.48 N/m2 for the mass flow rate of 0.163 kg/sec.

Table 8. Average values for selected days in May and June. 2021

day	Average solar radiation(w/m^2)	Average Ambient temperature (°C)
30 th	786.4	43.85
31st	796	44.125
1st	792.4	44.9
2 nd	777.4	42.725
3 rd	795.9	42
5 th	786	44.2

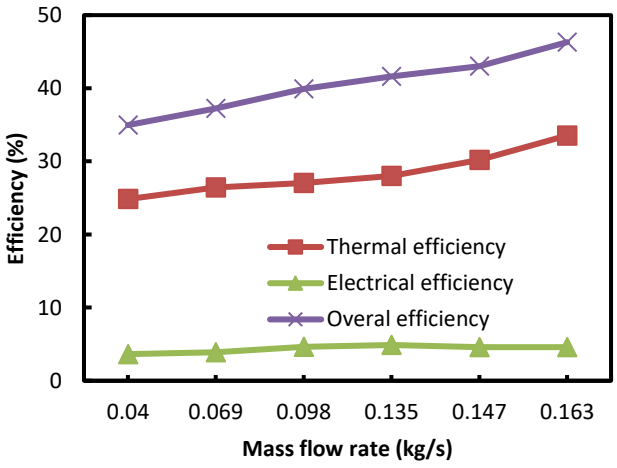

Figure 12. Variation of efficiency with mass flow rate

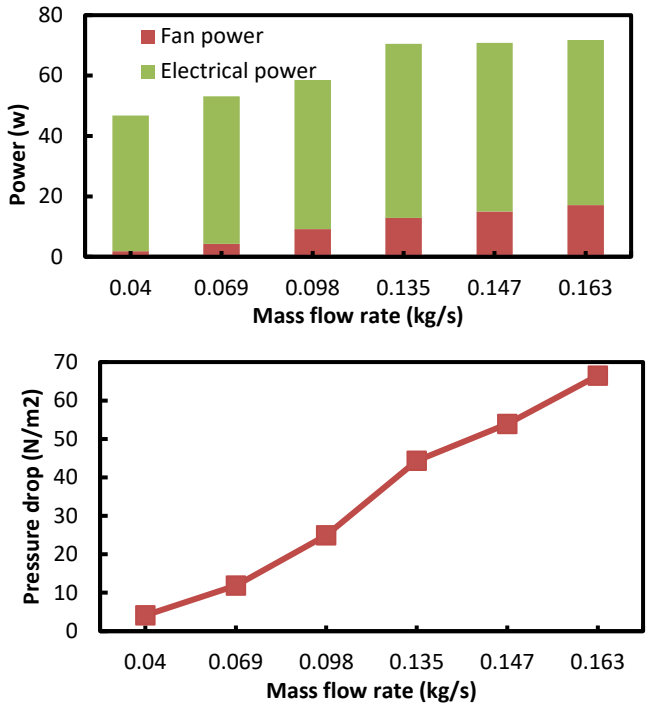

Figure 14. Variation of pressure drop with mass flow rate

9. Conclusion

The current study deals with the study of the hybrid collector (PV/T) to search for the optimal angle of the hybrid collector in the climatic conditions of Fallujah city and its impact on the electrical energy of solar panels. The current research also touched on the effect of changing the mass flow rate on electrical power and thermal and electrical efficiency, and concluded the following:

- It turns out that the best angle for the PV/T hybrid collector is 30°, which results in the most electrical power.
- As the angle of inclination increases, so does the incident solar radiation, which has a negative impact on hybrid collector performance due to the high temperature of the solar panels.
- Increasing the mass flow rate has no significant impact on electrical efficiency .
- Increasing the mass flow rate has no significant impact on electrical efficiency .
- Increasing the mass flow rate improves thermal efficiency and overall efficiency.

Nomenclature

A_s	Cross sectional area of channel (m^2)
A_p	Aperture area of collector (m^2)
A_{pv}	Total area of PV (m^2)
b	Width of channel (m)
C_f	Conversion factor of thermal power plant
Cp	Specific heat of air (J/kg.℃)
Dh	Hydraulic diameter of the air passage (m)
e	Root mean square of percentage deviation (%)
f	friction factor
G	Incident Solar radiation (w/m^2)
h	High of channel (m)
I	Circuit current (A)
I_{load}	Current of load (A)
$I_{Max.}$	Current at maximum power
L	Length of collector (m)
R	Electrical resistance (Ω)
T	Temperature (℃)
$T_{ave.cell}$	Average cell temperature (℃)
$T_{solar\ cell}$	Solar cell temperature (℃)
t	Time (s)
V	Circuit voltage (V)
V_a	Air velocity (m/s)
V_{load}	Voltage of load (V)
V_{max}	Voltage at maximum power
X	Simulated value of a variable parameter

y	Experimental value of a variable parameter

Greek symbols

ρ	Density (kg/m^3)
μ	Dynamic viscosity (kg/m s)
Δp	Drop pressure (N/m^2)
$\dot{m}$	Mass flow rate (kg/s)
n	Number of data
PV	Photovoltaic
PV/T	Photovoltaic/thermal
P_{fan}	Power of fan
P_{load}	Power of load
P_{pv}	Power of PV
Q_u	Heat gain (w)
r	Linear coefficient of correlation
η	Efficiency (%)

Subscript

amb	Ambient
ele	Electrical
in	Inlet
oc	Open circuit
sc	Short circuit
out	Outlet
th	Thermal

References

[1] A. S. Joshi, A. Tiwari, G. N. Tiwari, I. Dincer, and B. V. Reddy, "Performance evaluation of a hybrid photovoltaic thermal (PV/T) (glass-to-glass) system," *Int. J. Therm. Sci.*, vol. 48, no. 1, pp. 154–164, 2009, doi: 10.1016/j.ijthermalsci.2008.05.001.

[2] F. Sarhaddi, S. Farahat, H. Ajam, A. Behzadmehr, and M. Mahdavi Adeli, "An improved thermal and electrical model for a solar photovoltaic thermal (PV/T) air collector," *Appl. Energy*, vol. 87, no. 7, pp. 2328–2339, 2010, doi: 10.1016/j.apenergy.2010.01.001.

[3] A. Tiwari, M. S. Sodha, A. Chandra, and J. C. Joshi, "Performance evaluation of photovoltaic thermal solar air collector for composite climate of India," *Sol. Energy Mater. Sol. Cells*, vol. 90, no. 2, pp. 175–189, 2006, doi: 10.1016/j.solmat.2005.03.002.

[4] A. Kasaeian, Y. Khanjari, S. Golzari, O. Mahian, and S. Wongwises, "Effects of forced convection on the performance of a photovoltaic thermal system: An experimental study," *Exp. Therm. Fluid Sci.*, vol. 85, pp. 13–21, 2017, doi: 10.1016/j.expthermflusci.2017.02.012.

[5] K. E. Amori and H. M. Taqi Al-Najjar, "Analysis of thermal and electrical performance of a hybrid (PV/T) air based solar collector for Iraq," *Appl. Energy*, vol. 98, pp. 384–395, 2012, doi: 10.1016/j.apenergy.2012.03.061.

[6] K. E. Amori and M. A. Abd-AlRaheem, "Field study of various air based photovoltaic/thermal hybrid solar collectors," *Renew. Energy*, vol. 63, pp. 402–414, 2014, doi: 10.1016/j.renene.2013.09.047.

[7] O. K. Ahmed and Z. A. Mohammed, "Dust effect on the performance of the hybrid PV/Thermal collector," *Therm. Sci. Eng. Prog.*, vol. 3, pp. 114–122, 2017, doi: 10.1016/j.tsep.2017.07.003.

[8] L. pauly, L. Rekha, C. V. Vazhappilly, and C. R. Melvinraj, "Numerical Simulation for Solar Hybrid Photovoltaic Thermal Air Collector," *Procedia Technol.*, vol. 24, pp.

513–522, 2016, doi: 10.1016/j.protcy.2016.05.088.

[9] J. K. Tonui and Y. Tripanagnostopoulos, "Improved PV/T solar collectors with heat extraction by forced or natural air circulation," *Renew. Energy*, vol. 32, no. 4, pp. 623–637, 2007, doi: 10.1016/j.renene.2006.03.006.

[10] S. Dubey, G. S. Sandhu, and G. N. Tiwari, "Analytical expression for electrical efficiency of PV/T hybrid air collector," *Appl. Energy*, vol. 86, no. 5, pp. 697–705, 2009, doi: 10.1016/j.apenergy.2008.09.003.

[11] M. Fterich, H. Chouikhi, H. Bentaher, and A. Maalej, "Experimental parametric study of a mixed-mode forced convection solar dryer equipped with a PV/T air collector," *Sol. Energy*, vol. 171, no. May, pp. 751–760, 2018, doi: 10.1016/j.solener.2018.06.051.

[12] M. M. Ali, O. K. Ahmed, and E. F. Abbas, "Performance of solar pond integrated with photovoltaic/thermal collectors," *Energy Reports*, vol. 6, no. xxxx, pp. 3200–3211, 2020, doi: 10.1016/j.egyr.2020.11.037.

[13] O. K. Ahmed and Z. A. Mohammed, "Influence of porous media on the performance of hybrid PV/Thermal collector," *Renew. Energy*, vol. 112, pp. 378–387, 2017, doi: 10.1016/j.renene.2017.05.061.

[14] A. Hadipour, M. Rajabi Zargarabadi, and S. Rashidi, "An efficient pulsed- spray water cooling system for photovoltaic panels: Experimental study and cost analysis," *Renew. Energy*, vol. 164, pp. 867–875, 2021, doi: 10.1016/j.renene.2020.09.021.

[15] S. Jakhar, M. S. Soni, and N. Gakkhar, "An integrated photovoltaic thermal solar (IPVTS) system with earth water heat exchanger cooling: Energy and exergy analysis," *Sol. Energy*, vol. 157, pp. 81–93, 2017, doi: 10.1016/j.csite.2018.07.001.

[16] A. M. Ali Morad, A. K. S. Al-Sayyab, and M. A. Abdulwahid, "Optimisation of tilted angles of a photovoltaic cell to determine the maximum generated electric power: A case study of some Iraqi cities," *Case Stud. Therm. Eng.*, vol. 12, no. July, pp. 484–488, 2018, doi: 10.1016/j.csite.2018.07.001.

[17] A. K. Shaker Al-Sayyab, Z. Y. Al Tmari, and M. K. Taher, "Theoretical and experimental investigation of photovoltaic cell performance, with optimum tilted angle: Basra city case study," *Case Stud. Therm. Eng.*, vol. 14, no. September 2018, p. 100421, 2019, doi: 10.1016/j.csite.2019.100421.

[18] M. K. Sharma, D. Kumar, S. Dhundhara, D. Gaur, and Y. P. Verma, "Optimal Tilt Angle Determination for PV Panels Using Real Time Data Acquisition," *Glob. Challenges*, vol. 4, no. 8, p. 1900109, 2020, doi: 10.1002/gch2.201900109.

[19] R. J. Moffat, "Describing the uncertainties in experimental results," *Exp. Therm. Fluid Sci.*, vol. 1, no. 1, pp. 3–17, 1988, doi: 10.1016/0894-1777(88)90043-X.

[20] A. Shahsavar and M. Ameri, "Experimental investigation and modeling of a direct-coupled PV/T air collector," *Sol. Energy*, vol. 84, no. 11, pp. 1938–1958, 2010, doi: 10.1016/j.solener.2010.07.010.

[21] M. Al-Damook, Z. A. H. Obaid, M. Al Qubeissi, D. Dixon-Hardy, J. Cottom, and P. J. Heggs, "CFD modeling and performance evaluation of multipass solar air heaters," *Numer. Heat Transf. Part A Appl.*, vol. 76, no. 6, pp. 438–464, 2019, doi: 10.1080/10407782.2019.1637228.